Elsevier Editorial System(tm) for Engineering Geology
Manuscript Draft

Manuscript Number:

Title: Progressive shear-surface development in cohesive materials; implications for landslide behaviour

Article Type: Research Paper

Keywords: landslides
strain localisation
microcracks
failure
strain

Corresponding Author: Dr. Jonathan Martin Carey, PhD

Corresponding Author's Institution: GNS Science

First Author: Jonathan Martin Carey, PhD

Order of Authors: Jonathan Martin Carey, PhD; David N Petley , PhD

Abstract: The aim of this study was to investigate mechanisms of progressive shear surface development using a series of bespoke triaxial cell tests. Intact and remoulded samples of Gault Clay from the Ventnor Undercliff on the Isle of Wight in southern England were subjected to pore pressure reinflation testing in a triaxial cell, in which failure is generated by increasing pore pressure under a constant total stress state. In addition, a novel very long term (>500 days) creep test was undertaken, in which the sample eventually failed at a constant stress state below the failure envelope.

The experiments showed that undisturbed samples of the Gault Clay failed in a brittle manner, generating a linear trend when plotted using the Saito technique. On the other hand, remoulded samples showed ductile behaviour, as indicated by a non-linear Saito trend. A number of otherwise identical PPR tests were conducted in which the rate of increase in pore water pressure was varied. These tests showed strain rate generated at any point in the PPR tests depended on both the effective stress and the rate of change of effective stress. The latter is important because a change in stress generates a change in strain. Thus, whilst tests at different rates of change of effective stress are similar when plotted in q-p' space and in strain - p' space, they are markedly different in strain rate - p' space.

The long term creep test failed when the stress state had been constant for over 80 days. This mechanism was reminiscent of creep rupture, occurring below the failure envelope defined in the conventional experiments.

We conclude that first time failure in the Gault Clay is a progressive mechanism dominated by the development of micro-cracking, which leads to strain localisation and the development of one or more shear surfaces at failure. Whilst this mechanism may usually occur in response to a change in stress, the study indicates that failure can develop progressively. In the remoulded Gault Clay shear strains cannot localise along a singular shear surface.

The results provide new insight into the mechanisms of landslide movement operating within the Ventnor landslide complex and indicate that present movements are likely to be occurring on a pre-existing shear surface. The lab tests suggest that this material is unlikely to undergo catastrophic failure.

Suggested Reviewers: Murphy Bill PhD
Senior Lecutreer, Geology, Univeristy of Leeds
w.murphy@leeds.ac.uk
Expert in Engineering Geology and landslide mechanisms. Undertakes research on landslides and landslide behaviour in the UK.

Denys Brunsden PhD
brunsden@chideock.co.uk
An international expert on landslide geomorphology and landslide movement and a published author on the Ventor and Undercliff landslides.

Jordi Corominas PhD
Geotechnical Engineering, Polytechnic University Catalonia
International landslide expert

Michael Crozier PhD
Emeritus Professor, School og Geography Environment and Earth Science, Victoria University of Wellington
michael.crozier@vuw.ac.nz
International landslide expert

Vicki Moon PhD
Senior Lecturer, Earth and Ocean Sciences, Waikato University
Expert in geomechanics, engineering geology and soft rocks

Highlights

Highlights:

- Progressive shear surface development studied using specialist triaxial cell tests
- Provides new insight into mechanisms of landslide movement
- Experiments confirm brittle failure associated with shear surface development
- Creep test shows same failure mechanism occurs at constant stress
- Failure is progressive and results from micro-cracking and strain localisation

Progressive shear-surface development in cohesive materials; implications for landslide behaviour

J M Carey[1] and D N Petley[2]

[1] GNS Science, 1 Fairway Drive, Avalon, Lower Hutt 5010, PO Box 30368, New Zealand
[2] Department of Geography, Durham University, Durham, DH1 3LE, UK

ABSTRACT

The aim of this study was to investigate mechanisms of progressive shear surface development using a series of bespoke triaxial cell tests. Intact and remoulded samples of Gault Clay from the Ventnor Undercliff on the Isle of Wight in southern England were subjected to pore pressure reinflation testing in a triaxial cell, in which failure is generated by increasing pore pressure under a constant total stress state. In addition, a novel very long term (>500 days) creep test was undertaken, in which the sample eventually failed at a constant stress state below the failure envelope.

The experiments showed that undisturbed samples of the Gault Clay failed in a brittle manner, generating a linear trend when plotted using the Saito technique. On the other hand, remoulded samples showed ductile behaviour, as indicated by a non-linear Saito trend. A number of otherwise identical PPR tests were conducted in which the rate of increase in pore water pressure was varied. These tests showed strain rate generated at any point in the PPR tests depended on both the effective stress and the rate of change of effective stress. The latter is important because a change in stress generates a change in strain. Thus, whilst tests at different rates of change of effective stress are similar when plotted in q-p' space and in strain – p' space, they are markedly different in strain rate – p' space.

The long term creep test failed when the stress state had been constant for over 80 days. This mechanism was reminiscent of creep rupture, occurring below the failure envelope defined in the conventional experiments.

We conclude that first time failure in the Gault Clay is a progressive mechanism dominated by the development of micro-cracking, which leads to strain localisation and the development of one or more shear surfaces at failure. Whilst this mechanism may usually occur in response to a change in stress, the study indicates that failure can

develop progressively. In the remoulded Gault Clay shear strains cannot localise along a singular shear surface.

The results provide new insight into the mechanisms of landslide movement operating within the Ventnor landslide complex and indicate that present movements are likely to be occurring on a pre-existing shear surface. The lab tests suggest that this material is unlikely to undergo catastrophic failure.

1. INTRODUCTION

Progressive failure in landslides has been long identified (Terzaghi, 1950), and was conceptualised over 40 years ago (Bjerrum, 1967). The essence of the process for a simple translational landslide is that progressive failure requires time-dependent deformation of material forming the landslide shear surface (Federico *et al.,* 2004). Laboratory and field based studies undertaken by Varnes (1983) and others have shown that brittle landslide materials progress through three distinct phases of creep to failure, in common with separate observations within the damage-mechanics literature (Main, 2000 for example). In the latter case three-phase creep behaviour is conceptualised as being the result of contrasting strain hardening and strain weakening processes, in which strain hardening initially dominates but is subsequently superceded by strain weakening. In both the models and the laboratory observations a gradual decrease of the factor of safety (FoS) is observed as damage accumulates through time.

Despite these observations progress in understanding the relationships between material deformation and the resultant movement of a slope have been surprisingly limited, although some progress has been made in recent years (e.g. Voight, 1988; Iverson, 2005; Petley *et al.,* 2005a; 2005b; Liu, 2009; Ng and Petley, 2009; Ostric *et al.,* 2011). The renewed interest in this topic has been driven at least in part by the need for better models to underpin strategies to reduce the losses from, and to manage the risk posed by large, brittle landslides. In many cases, failure cannot be prevented due to the size of the unstable slope, the difficulty of accessing it and/or the potential cost of large-scale engineered interventions. Thus, recent research has focused on the development of an understanding of the mechanisms and processes of progressively failing landslides in order to allow predictions to be made for likely patterns of behaviour. In principle, such methods could provide powerful tools to underpin landslide warning systems.

The so-called ‘Saito approach’ (Saito, 1965), and its subsequent developments (Fukozono 1990 for example), has been the key technique for analysing progressive failure. The approach is based on the concept that the time to failure can been estimated by identifying a linear trend in inverse velocity (1/v, where v is velocity) - time space as the landslide approaches failure. Using this method, time to failure can be estimated from the extrapolation of the inverse velocity trend to zero (i.e. the point at which the velocity of the slope is theoretically infinite). Petley *et al.* (2002) and Kilburn and Petley (2003) linked the linear trend to micro-crack development and shear-surface development. This crack-propagation model provides a theoretical explanation of why, in brittle materials, the development of strain rate with time in a brittle material is a hyperbolic function (i.e. why it yields a linear trend in 1/v - t space, as the inverse rate of displacement changes linearly with time. An alternative model lies in the rate- and state-dependent friction (e.g. Helmstetter *et al* 2003), but the observation that non-brittle materials show a non-linear trend in 1/v – t space favours the crack-propagation model, and is also consistent with the model of Bjerrum (1967).

Whilst such methods have been successful as predictors for some slope failures (e.g. Voight, 1988; Fukuzono, 1990; Petley *et al.,* 2002), in general approximating the time to failure of landslides remains uncertain. This, in part, is because the physics controlling the deformation to failure has yet to be fully elucidated (Hutchinson, 2001a). The observations of Petley *et al.* (2002) and Petley and Petley (2006) suggest that the Saito technique is only applicable in brittle materials, which can yield a linear trend in 1/v, t space.

To determine the safety and future potential of landslide initiation and reactivation, a detailed understanding of the physical, hydrological and geotechnical properties of materials is essential (e.g. Varnes, 1978; Hutchinson, 1967; 1984; 2001b). However, generating laboratory-based geotechnical data that can be compared with field-based landslide monitoring records has remained complex. One significant limitation is that conventional geotechnical tests generate failure by increasing deviator stress at a constant displacement rate. Most rainfall-induced landslides occur as a result of increasing pore pressure acting within the slope, which reduces mean effective stress at approximately constant deviator stress. Thus, standard geotechnical tests are not well-suited to defining the true failure envelope in such conditions (Zhu and Anderson, 1998, Orense *et al.,* 2004)l although they are optimised for providing conservative strength parameters for design purposes.

A range of novel testing procedures have been developed to simulate failure conditions resulting from elevated pore pressures (Brand, 1981; Anderson and Sitar, 1995; Zhu and Anderson, 1998; Dai *et al*., 1999; Orense *et al.* 2004 for example). The key feature of these studies has often been the concept of increasing pore pressure within a sample at constant total normal stress and shear stress – the so-called "field" stress path, but termed by Petley *et al*. (2005a) and subsequent papers the pore pressure reinflation test (e.g. Petley *et al*., 2005b; Carey *et al.,* 2007; Ng and Petley, 2009). Whilst these tests have yielded useful results, their applicability to understanding landslide behaviour has been limited. Often the rationale behind rates of pore pressure reinflation has not been considered in detail and the system capabilities for controlling pore pressures and deviator stress acting on the sample have been inadequate. Interpretation of the results has often focussed on the form of the Mohr-Coulomb failure envelope. In addition, testing has focused largely on tropical and subtropical soils, which mainly comprise weathered soils subject to shallow failure (<5 m) in intense rainfall conditions. As a consequence testing has been skewed toward understanding residual-strength materials at low effective stresses and high rates of pore-pressure reinflation.

Further research is required to link movement patterns in both first-time landslides and reactivation failures to the patterns and mechanics of shear-surface development in cohesive materials, if accurate landslide-failure prediction and behaviour forecasting methods can be established. This paper aims to improve understanding by presenting a series of tests on both intact and remoulded samples of Gault Clay collected in the Ventnor Undercliff in the UK. The study replicates groundwater-induced landslide-failure conditions from a monitored landslide complex to study the patterns of deformation to failure under varying pore-pressure reinflation scenarios.

This provides new insights into the mechanism of shear-surface development and strain-induced failure in deep-seated landslide complexes.

2. SITE LOCATION

Ventnor is located on the south coast of the Isle of Wight (Fig 1), centred at 50°35'40.83N, 1°12'2162W. The Ventnor Undercliff is one of the largest landslide complexes in the United Kingdom (UK), with potential impacts on a population of over 6000 residents (Fig 2). A review of landsliding in the UK (GSL, 1987) identified the Ventnor Undercliff as the largest urban area affected by landsliding, such that it has been the subject of a number of previous studies (e.g. Chandler, 1984; Hutchinson *et al.,* 1991a, 1991b; Lee and Moore, 1991; Moore *et al.,* 1995; Hutchinson and Bromhead, 2002; Moore *et al.,* 2007a, 2007b). The Ventnor landslide complex covers an area of 0.7 km^2 (Fig 2 a), forming a deep-seated, complex landslide with a rotational component close to the crown and a translational component downslope. The rear of the landslide is delineated by a large, actively-developing depression known as the 'Lowtherville Graben' (Fig 2 a).

A succession of ground investigations at Ventnor have obtained geological information to a depth of up to 150 m below ground level in Upper Ventnor. More recent large-scale ground investigations were undertaken in 2002 (Soil Mechanics Ltd) and 2005 (Fugro Engineering Services Ltd), and included five deep rotary and open-cored boreholes; engineering and geophysical logging of materials; laboratory testing of samples; and installation of inclinometers and standpipe piezometers.

Moore *et al.* (2007a) used engineering and geophysical logs from the 2002 and 2005 investigations, and an earlier stratigraphic analysis (Lee and Moore, 1991), to develop description detailed understanding of the materials that form the landslide. A summary of the key units is provided in Figure 2b.

Inclinometer records (Fig 2 c) and the findings of the 2005 ground investigations were subsequently used to develop a landslide model for the Ventnor Undercliff (Moore *et al.,* 2007b), which hypothesises the presence of a retrogressive complex comprising distinct upper and lower landslide sections. In both cases, the sliding surface is located towards the base of the Gault Clay Formation.

The landslide complex is probably ancient, but continues to undergo continuous low magnitude deformation. Rates of movement are low (typically in the order of millimetres to centimetres per year) across the whole system, although locally higher rates are occasionally recorded. The rate of movement of the landslide increases during prolonged periods of high rainfall (Moore *et al.* 2010). Movements of the landslide can generate considerable damage to buildings and other infrastructure within the town, and there remains a great deal of interest in the likely long term behaviour of the landslide complex.

3. METHODS

For this study, a suite of laboratory tests has been used to determine the physical and geotechnical characteristics of the materials within the Ventnor landslide complex. The experiments used a series of isotropic, consolidated, undrained (ICU) triaxial tests to establish field-stress conditions, with specialist isotropically consolidated drained (ICD) PPR tests designed to simulate the porewater pressure conditions that may occur in the landslide during movement events.

83 mm diameter core samples taken from close to the known shear surface at the base of the Gault Clay in BH5 (Fig 3c), and hand-cut block samples from exposures of stratigraphic-equivalent Gault Clay from Blackgang Chine (Fig 2), were logged and recorded before being sealed on-site using cling film and wax. Samples were placed within plastic containers and carefully transported to the University of Durham.

An initial set of standard soil classification tests were undertaken on the Gault Clay to establish the physical properties of the landslide materials at the basal shear zone (Table 1). Particle-size analyses (Fig. 4) indicate some variability across the Gault Clay samples. Samples from BH5 comprised of 14.1% clay, with silt contents of 39.3% and sand content of 46.6%. Whilst similar silt contents can be observed in BS samples (39.3%), a lower clay content of 11.9% and a higher sand content of 47.7% were recorded. Plastic limits were similar in both samples, although liquid limits were significantly higher in BH5. Atterberg limits indicate that the Gault Clay samples comprise high plasticity clay in BH5 and low plasticity clay in BS (defined in accordance with BS5930, 1981). The natural moisture content in both samples was 17%.

Triaxial tests used a PC-controlled stress path triaxial testing system, designed and manufactured by GDS Instruments. The system used a classic Bishop and Wesley (1975) hydraulic stress path triaxial cell with a 38 mm diameter pedestal and top caps, one 4 kN submersible load cell and 50 mm-range displacement transducers. Four ICU tests (Table 2) and seven ICD PPR tests (Table 3) were completed. In all 11 tests, soil samples were initially saturated by flushing with carbon dioxide at a slow rate prior to saturation with de-aired water to fill pore air voids at a low initial confining pressure (BSI, 1990b). Samples were isotropically consolidated by increasing confining pressures at 1 kPa/hr to the required stress states. Consolidation was complete when no further significant volume change occurred and excess porewater pressure, associated with the stresses applied, had dissipated (BSI, 1990a).

Undrained samples ICU1, ICU2, ICU4 and ICU 6 were consolidated to initial confining pressures of 250, 350, 450 and 550 kPa respectively. Following consolidation, each sample was subjected to undrained shear at a rate of 0.001 mm/min to prevent the development of heterogeneous pore water pressures. The shear phase was undertaken in an undrained state but rates of strain were sufficiently slow to allow pore water pressures to equalibriate (BSI, 1990a).

Drained intact samples (ICD2, ICD6 and ICD7) and drained remoulded samples (ICDR1, ICDR2 and ICDR3) were carried out from an initial confining pressure of 350 kPa. The ICD and ICDR PPR samples were subject to an initial drained shear phase following consolidation at a displacement rate of 0.001 mm/min until a deviator stress of 400 kPa was achieved. Failure was then initiated at a constant deviator stress of 400 kPa by increasing the porewater pressure at reinflation rates of 5, 10 and 18 kPa/hr (Fig 5a and b). The rates of pressure reinflation were selected to replicate plausible groundwater recharge rates from the available Ventnor piezometric data (Moore *et al.,* 2010). During each PPR test, axial deformation was monitored using a displacement transducer located at the top of the sample. Porewater pressure measurements were recorded at the top and bottom of the sample.

An additional long-duration creep test was undertaken (ICD12) which aimed to study the potential for a shear surface to develop at a constant stress state (i.e. to simulate true progressive failure). In this test, the sample was subjected to the standard initial confining pressure of 350 kPa and initial drained shear of 400 kPa, in common with tests ICD2, 6 and 7. During the PPR stage, porewater pressure was incrementally increased in small steps before being held constant to study sample strain development (Fig 4c). As the test progressed, PPR phases were shortened and the constant PPR phases lengthened to determine whether strain development to failure could occur at constant mean effective stress (Fig 4 d).

4. RESULTS

The consolidation curves for both ICU (Fig 5a) and ICD (Fig 5b) tests on intact Gault Clay samples were constructed at confining pressures ranging from 250 kPa to 550 kPa. Whilst the results demonstrate some variability in behaviour between the samples, as expected there was a general trend of increased volumetric strain occurring in samples consolidated at higher mean effective stress. Consolidation curves from the ICDR test illustrated similar behaviour across the samples (Fig 5c), indicating the more consistent nature of the samples tested.

The ICU stress paths (Fig 6) showed variability in both peak and residual strength characteristics between the tests, indicative of the heterogeneous nature of the Gault Clay. As a consequence, laboratory data from a previous study at the site (Carey, 2002) has been included in the assessment of the strength parameters of the Gault Clay. The peak and residual strength envelopes suggest that the peak strength values of ø’ = 35.1° and c’ = 46.8 kPa (Fig 7 a), whilst residual strength is represented by ø’ = 26.6° and c’ = 0 kPa (Fig 7 b).

The ICD PPR tests on the intact Gault Clay showed two distinct phases of volume change in the samples (Fig 8a). During the early phases of the reinflation phase of the experiment the sample underwent dilation, with the rate of volume change being near linear with time in all three samples. In this initial period of deformation, corresponding displacement rates were low (Fig 8b). Note that the control system was applying a constant rate of pore pressure change, suggesting a simple dilation process. In all cases, this initial phase of movement was characterised by an exponential increase in displacement rate (Fig 8c) and an asymptotic trend in 1/v - t space (Fig 8d), consistent with the observations of Ng (2007) for residual soil. Thus, in this phase the bulk sample behaviour was similar to that of a ductile material, probably because strain localisation has not occurred, such that deformation is distributed through the sample. Note that displacement rates are very low and vary considerably in this phase; it is not clear as to whether this is noise or that the deformation is occurring through a 'stick-slip' type process (Allison and Brunsden, 1990).

As the pore pressure increased further, the rate of dilation in the samples increased (Fig 8a). The rate of increase of volume change with time is best described by a hyperbolic trend in all three samples (Fig 8b), which matches the hyperbolic acceleration to failure observed in the displacement rate data (Fig 8c). This yields a linear trend in 1/v – t space (Fig 8d), and is thus associated with strain localisation and the development of a shear surface (Kilburn and Petley 2003). Final failure in the samples was associated with the development of either a single shear surface,, or in some cases of a conjugate pair of shear surfaces

Remoulded Gault Clay samples also showed dilative behaviour during PPR testing, but the style of behaviour was notably different. Most importantly, in the early stages of reinflation the rate of dilation was higher than for the undisturbed samples (which is consistent with the material being weaker). However, in the latter stages of the test the dilation rate was lower than the corresponding rate for the undisturbed sample, even though there was an accelerating trend. For the remoulded samples the rate of change of volume with time is best described by an exponential trend (Fig 9b), in common with the displacement rate – time data (Fig 9c). In the remoulded samples, strain did not localise to form a shear surface, with deformation remaining distributed through the sample. As a consequence a linear trend in 1/v –t did not develop and instead deformation continued along an asymptotic trend (Fig 9d).

Thus, the hyperbolic increase in both dilation rate and displacement rate with time during reinflation is associated with the structure of the undisturbed Gault Clay. When the structure is destroyed in the remoulded samples the behaviour is lost. Thus, the behaviour is a characteristic of the strain localisation process.

Whilst PPR testing demonstrated the significance of material properties on the mechanisms of deformation, the linear increases in pore-pressure reinflation used in these tests do not perfectly replicate landslide conditions. In particular, by forcing the sample to fail under a linearly-reducing effective stress state the test may mask time-dependent failure mechanisms associated with progressive shear-surface development at constant stress. To investigate this, a long-creep test was undertaken during which pore-water pressures were raised, initially in increments of 10 kPa, and latterly of 2 kPa. After each increase the pore pressure was held constant to allow for any initial volumetric or strain response in the sample to develop before the next increment was applied. In this way, failure occurred whilst the sample was at a constant stress state after the test had run for 524 days (Fig 10a). In the final phase of the test, the pore pressure was increased on day 444 thereafter it was kept constant for 81 days until failure occurred.

During the final 80 days the sample crept to failure at a constant effective stress (Fig 10bi). As failure developed in the sample, strain developed constantly, but some notable stepped increases (Fig. 10bi) that were not associated with a change in effective stress state. The rate of occurrence of these five steps does not increase towards failure, suggesting that they are not precursors to the final failure event. Note however that they are associated with a change in sample volume; in each case there was a small amount of dilation (Fig. 10bii).It is unclear as this stage as to whether stepped pattern results of a stick-slip process or is a function of the test.

Final failure was initiated at Day 78 of this final stage of the experiment. The sample underwent a hyperbolic acceleration in rate of volume change with time and rate of displacement with time during the final few days (Fig 10 ci and ii). Final failure occurred at mean effective stress of approximately 187.5 kPa, which plots below the failure envelope derived from both the conventional and the PPR tests.

Analysis of the final 11 days of the test suggests that the sample dilated during deformation (Fig 10 ci), similar to that observed in the ICU PPR tests. The displacement rate was constant and acceleration to failure did not develop until day 78 (Figure 10 cii and 10 ciii). Analysis of the final four days (day 78 to day 81) suggests rapid development of a shear surface during the final day of the test as the sample dilated (Fig 10 di,) and displacement rate rapidly developed into a hyperbolic trend (Fig 10 dii). This is illustrated by the linearity in 1 / v, t space observed over the final four days (Fig 10 diii). The test indicates that whilst damage is occurring throughout the sample, the acceleration to failure resulting from strain localisation occurred very rapidly and very late in the deformation process.

5. DISCUSSION

A suite of pore pressure inflation tests have been undertaken to study the mechanisms of deformation to failure under a series of representative pore water pressure-induced landslide scenarios. The study has demonstrated that the patterns of deformation and the condition of the shear surface during failure vary depending on the rate of pore pressure increase and the nature of the existing shear surface.

In Figure 11a, the displacement during the PPR phase of the three undisturbed tests, plus the long term creep test, is shown against mean effective stress. The intact Gault Clay shows a progressive brittle failure mechanism as a result of the development of a singular shear surface through the process of strain localisation. For the three PPR tests the behaviour is the same within error. The long term creep test fails at a higher mean effective stress, consistent with the creep rupture results of Singh and Mitchell (1969). The PPR testing indicates that displacement in intact samples of the Gault Clay initiated from a mean effective stress of approximately 300 kPa (Fig 11 a). Final failure appears to occur at a critical displacement rather than a critical stress state.

In the PPR tests, a similar relationship, within error, is observed between displacement and mean effective stress. This means that the displacement –time relationship varies between the experiments according the rate of pore pressure increase (Fig 11b). Thus, the rate of strain at any point in time is dependent upon both the effective stress state and the rate of change of effective stress. It is notable that whilst the 10 and 18 kPa / hr tests showed very similar behaviour, the 5 kPa per hour test developed displacement at higher effective stress values, and failed at a higher effective stress state, although its post failure behaviour was similar to that of the other two tests.

The progressive development of failure is a non-linear process. In these tests the increase in displacement with changing effective stress is an exponential relationship. Plotted in 1/v - t space, linearity is observed from approximately 200 kPa in all samples (Fig 11c), indicating that the critical point in terms of development of the shear surface occurs at or close to this effective stress value. Prior to this point deformation is dominated by sub-critical crack growth throughout the sample, but with increasing localisation around the proto-shear surface. After this point, strain localisation has occurred and the shear surface is rapidly developing.

The long term creep test shows notably different behaviour. Note that in this test effective stress was reduced in small steps, after which the sample was allowed to develop strain. The result is that the sample shows a much great level of displacement for any given effective stress value. Inevitable this style of testing induces a step-wise pattern in the dataset, but nonetheless the overall pattern of deformation prior to final failure is exponential against mean effective stress state.

The most important observation is that final failure occurred at a much higher value of mean effective stress than was the case for the linear PPR tests. The 5 kPa / hr test failed at a stress state that is consistent with the ICD failure envelope. The 10 and 18 kPa / hour tests failed at a lower effective stress state, suggesting slightly stronger materials. However, this may also indicate a lack of pore pressure equalisation through the sample (i.e. that the effective stress state in the shear zone was higher than is indicated by the pore pressure measurements at ends of the samples). However, the long term creep test suggests a weaker failure envelope than the ICU tests would imply (Fig 12 b). This cannot be due to a lack of pore pressure equalisation in this case. It is also notable that final failure developed in conditions of constant mean effective stress (Fig. 10); indeed, final failure occurred 81 days after the pore pressures had last been changed. Creep-rupture behaviour is observed in crystalline rock s with deviator stress states below the peak strength. It is a time-dependent process associated with progressive damage accumulation in the sample. The time to failure is inversely correlated with the deviator stress – thus samples in a stress state close to the failure envelope will fail comparatively rapidly; those at lower levels of deviator stress will fail more slowly. Thus, in effect creep-rupture defines a suite of failure envelopes below the ICD envelope. In crystalline rocks these are generally parallel or sub-parallel to the failure envelope, suggesting that the peak effective friction angle is unchanged, but that creep rupture leads to a reduction in cohesion.

The implications of this observation for brittle landslides are key. Most importantly, the creep rupture process can allow a landslide to fail at an effective stress state that is higher than that suggested by ICD tests. In addition, the long term creep tests suggest that in a creeping landslide with brittle deformation processes, failure can occur without a trigger, controlled instead by the progressive development of the shear surface. This is consistent with the observation of many deep, catastrophic rockslides (e.g. McSaveney, 2002) which appear to fail spontaneously. Shallow landslides also sometimes display this behaviour, especially when failure is observed days or weeks after the apparent trigger event, but these landslides tend to be in a much more dynamic stress state, and thus are more likely to fail through conventional triggered failure mechanisms.

Thus, creeping landslides in a brittle regime can undergo failure as a result of creep rupture processes without a trigger. However, in such cases they are likely to undergo precursory activity. In the long term this is in the form of evolving creep-type deformation; in the period leading to failure this will be a rapidly developing displacement rate that can be characterised as a linear trend in 1/v - t space.

The remoulded samples deformed to failure through ductile deformation, consistent with previous PPR testing observations on non-cohesive soils (Ng and Petley, 2009). In the remoulded tests deformation initiated at or close to the residual strength envelope. Behaviour was notably different from that of the undisturbed samples, suggesting that the creep-rupture behaviour is a brittle phenomenon. During the initial, slow phase of movement in the remoulded samples, minor changes in the displacement rate occur indicating a ‘push and climb’ mechanism of deformation previously observed by Ng and Petley, (2009). As mean effective stress continues to reduce, displacement rate increases as ‘localised sliding’ occurs as the frictional resistance of the shear surface progressively reduces through both internal deformation and increasing pore water pressure. As the mean effective stress continues to reduce further, soil particles within the shear zone progressively mobilise until generalised interparticular sliding throughout the sample. At this stage, displacement continues to accelerate exponentially and ductile failure occurs without the development of a singular shear surface. This is illustrated by an asymptotic trend in 1/v - p’ space throughout the test (Fig 11 d).

The laboratory testing further provides a new insight into the current and potential future behaviour of the Ventnor landslide complex. Landslide movement patterns have been shown to occur as a continual, very slow creep-type through time, with phases of accelerated ground movement which occur when pore water pressures are sufficiently elevated (Moore *et al.,* 2007a). PPR testing has confirmed that first time failures in the Gault Clay occur under a brittle deformation and, as a consequence, are less likely to be subject to significant levels of displacement prior to failure. However, in this initial failure event, which will occur successively in new rotational blocks at the rear of the landslide, catastrophic failure and rapid movement, is prevented by the blocks downslope. The current movement across the majority of the landslide is likely to represent post-failure creep along a pre-existing landslide shear surface. Under groundwater induced conditions, therefore, the landslide is likely to remain marginally stable. Accelerated ground creep however is likely to occur when pore water pressures acting at the shear surface are sufficiently elevated to overcome the frictional strength acting at the shear surface. In view of this post failure behaviour, catastrophic failure of the landslide controlled by material properties is not considered likely. Profound weakening of the landslide system through a change in state of the lowest constraining block could have a marked effect and thus should be avoided. The Lowtherville Graben may indicate a brittle failure mechanism at the rear of the landslide, but rapid failure is not likely here due to the constraint imposed by the large downslope blocks.

7. CONCLUSIONS

The mechanisms of landslide shear surface development have been studied through a novel series of pore-pressure reflation (ICD PPR) tests on both intact and remoulded Gault Clay samples designed to replicate plausible field failure conditions.

The study has demonstrated that progressive development of first time landslide failure is a complex process as the displacement –time relationship varies between the experiments according the rate of pore pressure increase. As a consequence, the rate of strain at any point in time is dependent upon both the effective stress state and the rate of change of effective stress. Final acceleration to failure develops at the same mean effective stress, indicating that this represents critical point in terms of development of the shear surface where singular shear surface rapidly develops. Prior to this point deformation is dominated by sub-critical crack growth which is distributed throughout the slope, but with increasing localisation around the proto-shear surface. This creep rupture process can allow a landslide to fail at an effective stress state that is either higher or lower than the short-term failure envelope. In landslides where long-term brittle creep can develop, failure can occur without a trigger and controlled instead by the progressive development of the shear surface.

In slopes where the brittle failure mechanism cannot operate (e.g. non-cohesive soils and pre-existing landslides) creep movement is initiated at or close to the residual strength envelope and increases with reducing mean effective stress as the frictional resistance of the shear surface progressively reduces through both internal deformation and increasing pore water pressure.

The study provides a new insight into the behaviour of the Ventnor landslide complex indicating that whilst future retrogression of the Lowtherville Graben may be undergoing brittle failure at the rear of the landslide, rapid failure is not likely due to the constraint imposed by the large downslope blocks. Under groundwater induced conditions, therefore, the landslide is likely to remain marginally stable. Accelerated ground creep however is likely to occur when pore water pressures acting at the shear surface are sufficiently elevated to overcome the frictional strength acting at the shear surface.

8. ACKNOWLEDGEMENTS

The results presented in this paper are the product of collaborative PhD research between Halcrow, a CH2M-HILL Company, and the University of Durham. The research has been was funded, in part, through the Halcrow Award Scheme. The authors acknowledge the work and support of the Isle of Wight Council which has invested significantly in the continued monitoring and maintenance of the Ventnor Landslide Management Strategy to which they have allowed access. This manuscript has greatly improved following review comments from Dr Mauri McSaveney and Dr Nicola Litchfield.

REFERENCES

Allison, R. and Brunsden, D., 1990. Some mudslide movement patterns. Earth Surface Processes and Landforms, 15: 297-311.

Anderson, S.A. and Sitar, N. 1995. Analysis of rainfall induced debris flows, Journal of Geotechnical Engineering. American Society of Civil Engineers. 121. 544-552.

Bishop, A.W. and Wesley, L.D. 1975. A hydraulic triaxial apparatus for controlled stress path testing. Geotechnique, 25(4): 657-670.

British Standards Institute (BSI).1981. Code of Practice for Site Investigations. BS 5930: 1981.

British Standards Institute (BSI).1990a. British Standard Methods of Test for Soils for Civil Engineering Purposes. Part 1: General Requirements and Sample Preparation. BS 1377: Part 1.

British Standards Institute (BSI). 1990b. British Standards Methods of Test for Soils for Civil Engineering Purposes. Part 8: Shear strength tests (effective stress). BS 1377: Part 8.

Bjerrum, L. 1967. Progressive failure in slopes of over-consolidated plastic clay and clay shales. Journal of the Soil Mechanics Foundation Division of the American Society of Civil Engineers, 93: 1-49.

Brand, E.W., (1981). Some thoughts on rain-induced slope failure. Proceedings 10th International Conference on Soil Mechanics and Foundation Engineering, San Francisco. Balkkema. Pp. 2541-2578.

Carey, J.M. 2002. Determining Landslide behaviour through the Analysis of Landslide Movement Patterns and Material Geotechnical Properties. The Undercliff, Isle of Wight. MSc Dissertation (unpublished), University of Durham.

Carey, J.M., Moore, R., Petley, D.N. and Siddle, H.J. 2007. Pre-failure behaviour of slope materials and their significance in the progressive failure of landslides. In: R McInnes, J Jakeways, H Fairbank, and E Mathie (Editors), Proceedings of the International Conference Landslides and Climate Change, Ventnor Isle of Wight. Taylor & Francis, London. pp. 207-215.

Chandler, M.P. 1984. The Coastal landslides forming the Undercliff of the Isle of Wight. Ph. D. Thesis (unpublished), Imperial College, University of London.

Dai, F.C., Lee, C.F., Wang, S.J. and Feng, Y.Y., 1999. Stress-strain behaviour of a loosely compacted volcanic-derived soil and its significance to rainfall-induced fill slope failures. Engineering Geology, 53: 359-370.

Federico, A., Popsecu, M., Fidelibus, C. And Interno, G. 2004. On the prediction of the time of occurrence of a slope failure: a review: In W.A. Lacerda, M. Ehrlich, S.A.B. Fontoura and A.S.F. Sayao (Editors), Landslide: Evaluation and Stabilization. Proceedings of the 9^{th} International Symposium on Landslides, Rio de Janeiro, June 28-July 2, 2004. Leiden: A.A. Balkema, pp. 979-1188.

Fukuzono, T. 1990. Recent studies on the time prediction of slope failures. Landslide News, 4: 9-12.

Geomorphological Services Limited. 1987. Review of research into landsliding in Great Britain: Series E, National summary and recommendations. Technical report to Department of the Environment.

Helmsetter, A., Sornette, D., Grasso, J.R., Anderson, V., Gluzman, S. and Pisarenko, v. 2003. Slider-block friction model for landslides: implications for prediction of mountain collapse. Journal of Geophysical Research, 109 (B02): 210-225.

Hutchinson, J.N. 2001a. The Fourth Glossop Lecture, Reading the ground: morphology and geology in site appraisal. Quarterly Journal of Engineering Geology and Hydrogeology, 34: 7-50.

Hutchinson, J.N. 2001b. Landslide risk- to know, to foresee, to prevent, Geologia Tecnica and Abientale, 9: 3-24.

Hutchinson, J.N. 1984. Landslides in Britain and their counter measures, Journal of Japan Landslide Society. 12:1-25.

Hutchinson, J.N. 1967. The free degradation of London Clay cliffs. Proceedings of the Geotechnical Conference , Oslo, 1. pp.113-118.

Hutchinson, J.N. and Bromhead, E.N. 2002. Keynote Paper: Isle of Wight landslides. In: R.G McInnes and J Jakeways (Editors), Instability Planning and Management: Seeking Sustainable Solutions to Ground Movement Problems, Proceedings of International Conference, Ventnor. Thomas Telford: London, pp. 3-70.

Hutchinson, J.N., Bromhead, E.N. and Chandler, M.P. 1991a. Investigations of the landslides at St Catherines Point, Isle of Wight. In: R.J Chandler (Editor), International Conference on Slope Stability Engineering-Development and Applications, London: Thomas Telford. pp. 213-218.

Hutchinson, J.N., Brunsden, D. and Lee, E.M. 1991b. The geomorphology of the landslide complex at Ventnor, Isle of Wight. In: R.J. Chandler (Editor) International Conference on Slope Stability Engineering- Developments and Applications, London: Thomas Telford. pp. 157-168.

Iverson, R.M. 2005. Regulation of landslide motion by dilatancy and pore pressure feedback. Journal of Geophysical Research. 110(F2): Article no - F02015.

Kilburn, C.J. and Petley, D.N. 2003. Forecasting giant, catastrophic slope collapse: lessons from Vajont Northern Italy. Geomorphology. 54: 21-32.

Lee, E.M. and Moore, R. 1991. Coastal Landslip Potential Assessment: Isle of Wight Undercliff, Ventnor, Technical Report, Department of the Environment.

Liu, C.-N. 2009. Progressive failure mechanism in one-dimensional stability analysis of shallow slope failures. Landslides, 6: 129-137.

Main, I.G., 2000 . A damage mechanics model for power-law creep and earthquake aftershock and foreshock sequences. Geophysical Journal International, 142(1): 151-161.

McSaveney, M.J. 2002. Recent rockfalls and rock avalanches in Mount Cook National Park, New Zealand. Geological Society of America, Reviews in Engineering Geology. XV: 1-36.

Monma, K., Kojima, S, and Kobayashi, T. 2000. Rock slope monitoring system and rock fall prediction. Landslides News, 13: 33-34.

Moore, R. Lee, E.M. and Clark, A.R. 1995. The Undercliff of the Isle of Wight: a review of ground behaviour. Cross Publishing: London.

Moore, R., Carey, J.M., McInnes, R. G. and Houghton, J.E.M. 2007a. Climate Change, so what? Implicactions for ground movement and landslide event frequency in the Ventnor Undercliff, Isle of Wight. In: R.J McInnes, J Jakeways, H Fairbank and E Mathie (Editors), Proceedings of the International Conference Landslides and Climate Change, Ventnor Isle of Wight. Taylor & Francis, London. pp. 335-344.

Moore, R., Turner, M.D., Palmer, M.J. and Carey, J.M. 2007b. The Ventnor Undercliff: Landslide model, mechanisms and causes, and the implications of climate change induced ground behaviour risk. In: R. J McInnes., J Jakeways., H Fairbank, and E Mathie (Editors), Proceedings of the International Conference Landslides and Climate Change, Ventnor Isle of Wight. Taylor & Francis, London. pp. 365-375.

Moore, R., Carey, J.M. and McIness, R.G. 2010. Landslide behavior and climate change: predictable consequences for the Ventnor Undercliff, Isle of Wight. Quarterly Journal of Engineering Geology and Hydrogeology, 43, 447-460.

Ng, K-Y. 2007. Mechanisms of Shallow Rainfall Induced Landslides in residual Soils in Humid Tropical Environments. Thesis (Unpublished), University of Durham.

Ng, K-Y. and Petley, D.N. 2009. The use of pore pressure reinflation testing in landslide management in Hong Kong. Quarterly Journal of Engineering Geology and Hydrogeology. 42:487-498.

Orense, R., Farooq, K. and Towhata, I. 2004. Deformation behaviour of sandy slopes during rainwater infiltration. Soils and Foundations, 44(2): 15-30Brand, 1981; Anderson and Sitar, 1995

Ostric, M., Sassa, K., He, B., Takara, K, and Yamashiki, Y. 2011. Portable ring shear apparatus and its application. Proceedings of the Second World Landslide Forum, 3-7 October 2011, Rome.

Petley, D.N., Higuchi, T., Petley, D.J., Bulmer, M.H. and Carey. J., 2005a. The development of progressive landslide failure in cohesive materials. Geology, 33(3): 201-204.

Petley, D.N., Higuchi, T., Dunning, S., Rosser, N.J., Petley, D.J., Bulmer, M.H. and Carey, J., 2005b. A new model for development of movement in progressive landslides. In: O Hungr, R Fell, R Couture and E Eberhardt (Editors), Landslide Risk Management, A.T. Balkema, Amsterdam. pp. 201-204.

Petley, D.N., Mantovani, F., Bulmer, M.H. & Zannoni, A. 2005c. The use of surface monitoring data for the interpretation of landslide movement patterns. Geomorphology, 66:133-147.

Petley, D.N. and Petley, D.J., 2006. On the initiation of large rockslides: perspectives from a new analysis of the Vaiont movement record. In: S.G Evans, G S Mugnozza, A Strom and R.L Hermanns (Editors), Landslides from Massive Rock Slope Failure. NATO Science Series IV: Earth and Environmental Sciences. Springer: Dordrecht. pp. 77-84.

Petley, D.N., Bulmer, M.H. and Murphy, W. 2002. Patterns of movement in rotational and translational landslides. Geology. 2002;30:719-722.

Saito, M. (1965). Forecasting the time and occurrence of a slope failure. Proceedings of the 6th International Conference on Soil Mechanics and Foundation Engineering. 2. pp. 537-541.

Singh, A. and Mitchell, J.K. 1969. Creep potential and creep rupture of soils, Proceedings of the 7th International Conference on Soil Mechanics and Foundation Engineering, Vol 1, Sociedad Mexicana de Mecanica de Suelos, Mexico City, Mexico. pp. 379-384.

Terzaghi, K., 1950. Mechanisms of landslides. In: Geological Society of America (Editors), Application of Geology to Engineering Practice: Geological Society of America, New York. pp. 83-123.

Varnes, D.J. 1983. Time-deformation relations in creep to failure of earth materials. Proceeding of the 7th Southeast Asian Geotechnical Conference, 22-26, November 1982, Hong Kong. pp. 107-1302.

Varnes, D.J. 1978. Slope movement types and processes. In: R Schuster and R Krizek (Editors), Landslide Analysis and Control. Special Report 176. National Research Council (U.S). Transportation Research Board., National Academy of Sciences, Washington, D.C. pp. 11-33.

Voight, B. 1988. A relation to describe rate dependent material failure. Science, 243, 200-203.

Zhu, J.-H. and Anderson, S.A., 1998. Determination of shear strength of Hawaiian residual soil subjected to rainfall-induced landslides. Geotechnique, 48(1): 73-82.

FIGURE CAPTIONS

Figure 1. The location of the Ventnor Undercliff, Isle of Wight, UK

Figure 2. Schematic interpretation of the Ventnor landslide complex: (a) Map of the extent of the landslide complex, including the section line. Note the intensely urbanised nature of the landslide. (b) Schematic cross-section through the landslide, showing the multiple landslide blocks and the low angled shear surface; (c) inclinometer data showing the clear deformation at the sliding surface, located in this case at about 95 m below the ground level.

Figure 3. The particle size distribution of the Gault Clay samples from Block Sample (BS) and Borehole 5 (BH5)

Figure 4. The design of the PPR tests following the drained initial shear phase (a) pore pressure vs time plot for the PPR tests (b) Mean normal effective stress vs time plot for the PPR tests (c) pore pressure vs time plot for the long creep test (d) Mean normal effective stress vs. time for the long creep test.

Figure 5. Change in volumetric strain through time during consolidation for: (a) the ICU tests; (b) the ICD intact tests; and (c) the ICD remoulded tests.

Figure 6. Undrained shear stress paths, including additional Gault Clay ICU stress paths from Carey (2002) to allow definition of the failure envelope.

Figure 7. ICU Mohr Coulomb failure envelopes: (a) the peak strength envelope; and (b) the residual strength envelope.

Figure 8. ICD linear PPR test results for the undisturbed samples: (a) Change in sample volume vs time; (b) displacement rate against time; and (c) 1/ velocity vs. time:

Figure 9. ICD linear PPR test results for the remoulded samples: (a) Change in sample volume v. time; (b) displacement rate against time; and (c) 1/ velocity vs. time.

Figure 10. The results of the long term creep test: (a) displacement and porewater pressure vs time over the full duration of the PPR phase of the experiment (524 days); (bi) displacement and porewater pressure vs time for the final 81 days; (bii) Displacement rate and change in sample volume vs time for

the last 81 days; (ci) Change in sample volume vs. time for the last 11 days; (cii) Displacement rate vs. time for the last 11 days; (di) Change in sample volume vs time for the last 24 hours of the test; (dii) Displacement rate vs time for the last 24 hours of the test; (diii) 1/ velocity vs time for the last 24 hours of the test.

Figure 11. Comparison of ICD linear PPR and Long Creep PPR behaviour: (a) Displacement vs mean effective stress (p'); (b) Displacement vs pore water pressure; (c) 1/velocity vs mean effective stress (p') for the ICD linear PPR tests.

Figure 12. (a) Comparison of ICDPPR and PPR long creep failure points in relation to the short-term ICU failure envelope (b) Comparison of ICD PPR and PPR long creep failure envelopes in relation to the short-term ICU failure envelope.

Table Captions

Table 1. Physical properties of the Gault Clay samples.

Table 2. The isotropic consolidated undrained (ICU) tests undertaken in this research programme.

Table 3. The isotropic consolidated drained (ICD) pore pressure reinflation (PPR) tests undertaken in this research programme.

Table 1. Physical properties of the Gault Clay samples

Sample location	BS	BH5
Particle size:		
Sand (%)	47.70	46.61
Silt (%)	40.40	39.28
Clay (%)	11.90	14.10
Specific gravity (Gs)	2.70	2.73
Loss on Ignition (%)	3.69	5.02
Mc (%)	17	17
Liquid limit (%)	30.11	56
Plastic limit (%)	21.18	21
Plasticity index	8.93	35
Bulk density (mg/ m³)	2.069-2.21	2.069
Dry density (Mg / m³)	1.702-1.911	1.66

Table 2. Isotropic consolidated undrained (ICU) tests

Test Reference	Material	Confining pressure (kPa)	Strain rate during shear	PPR rate (kPa/hr)	Sample condition
ICU1	Gault	250	0.01	N/A	intact
ICU2	Gault	350	0.01	N/A	intact
ICU4	Gault	450	0.01	N/A	intact
ICU6	Gault	550	0.01	N/A	intact

Table 3. Isotropic consolidated drained (ICD) pore pressure reinflation (PPR) tests

Test Reference	Material	Confining pressure (kPa)	Stress path (kPa)	Initial Strain rate (mm/ min)	PPR rate (kPa/hr)	Sample condition
ICD2	Gault	350	400	0.01	10	intact
ICD6	Gault	350	400	0.01	18	intact
ICD7	Gault	350	400	0.01	5	intact
ICDR1	Gault	350	400	0.01	10	remoulded
ICDR2	Gault	350	400	0.01	18	remoulded
ICDR3	Gault	350	400	0.01	5	remoulded
ICD12	Gault	350	400	0.01	Long creep	intact

Figure 1
Click here to download Figure: 14_02 Carey JM_Fig_1.pdf

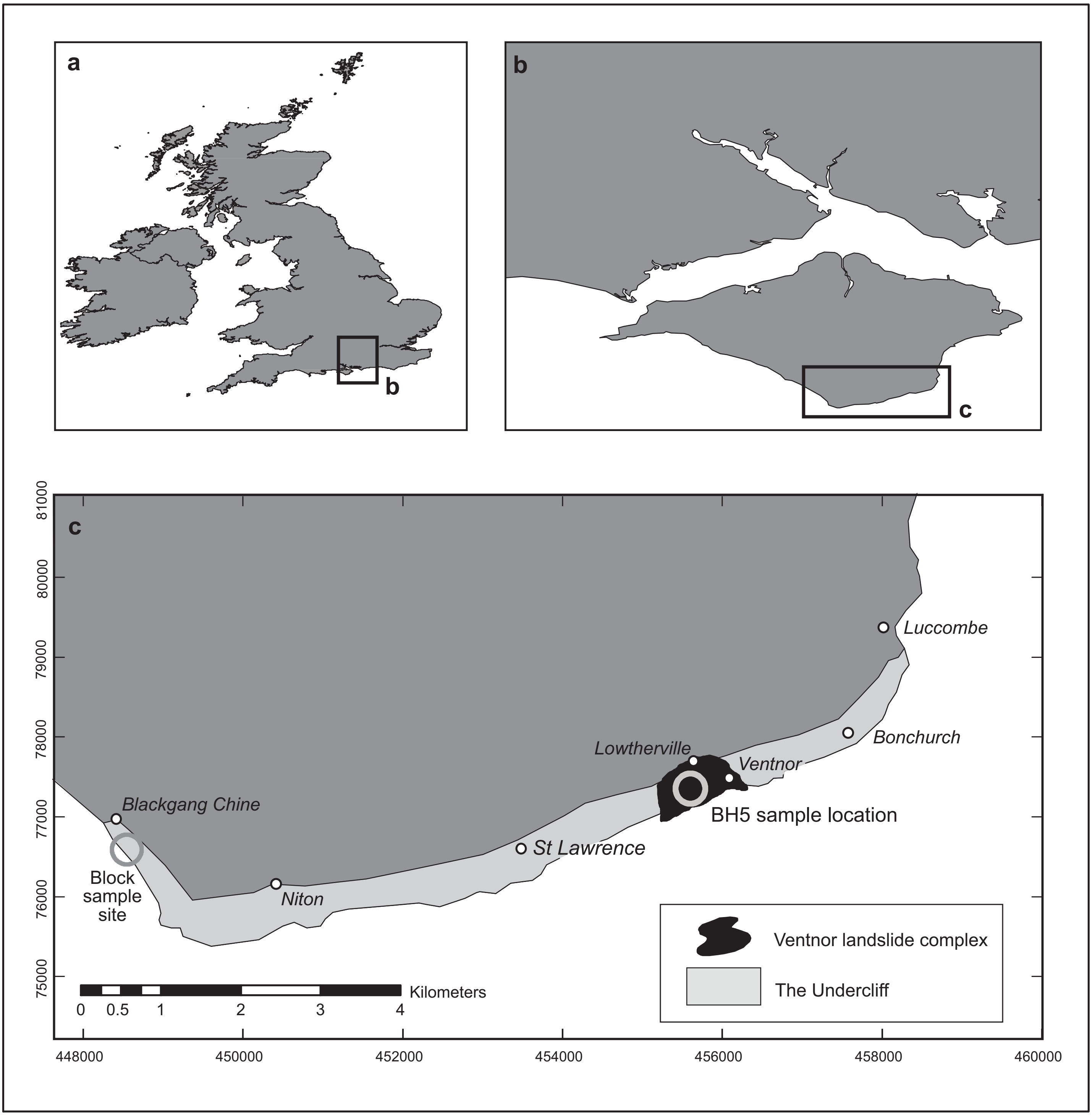

Figure 1

Figure 2
Click here to download Figure: 14_02 Carey JM_Fig_2.pdf

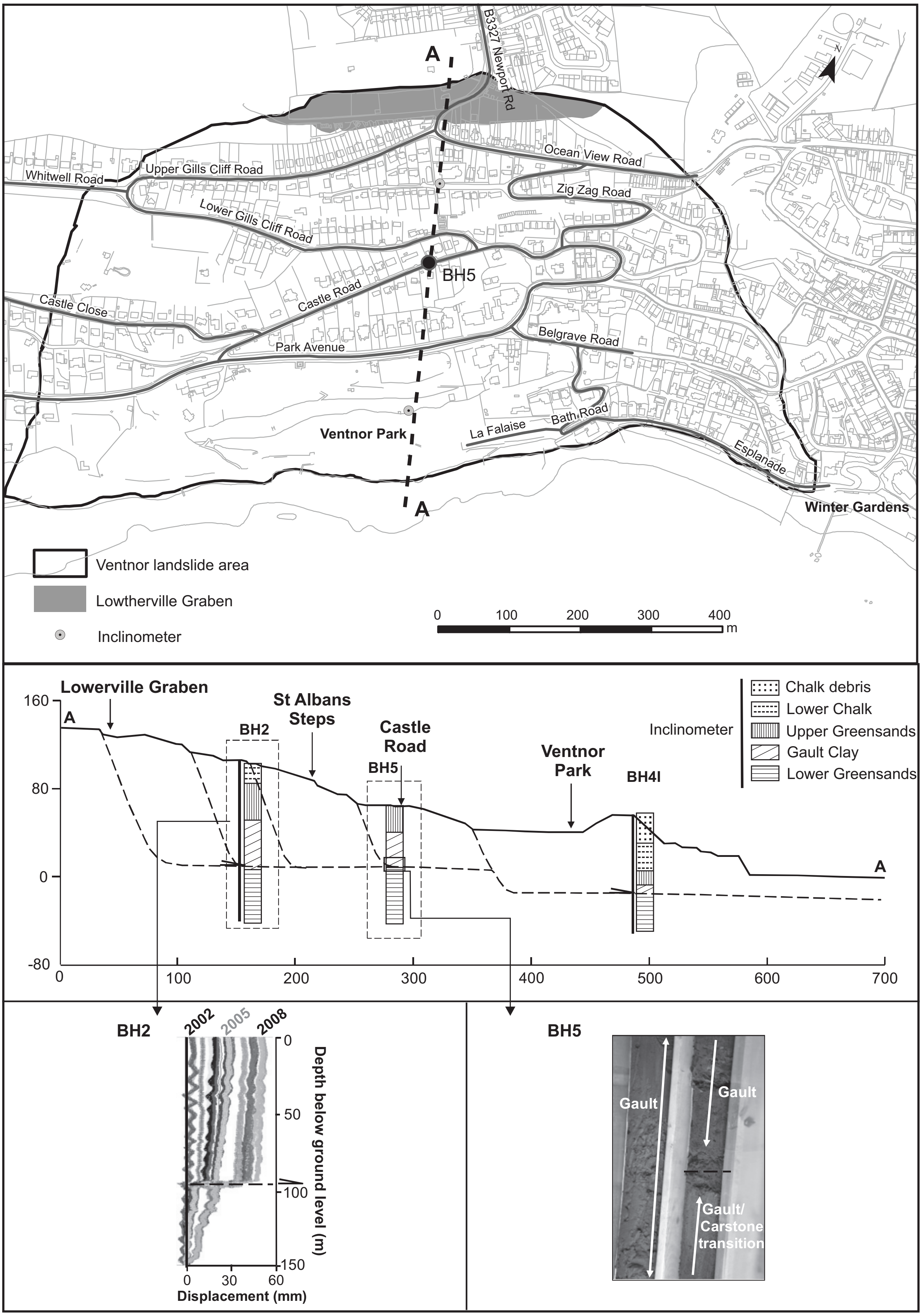

Figure 2

Figure 3

Click here to download Figure: 14_02 Carey JM_Fig_3.pdf

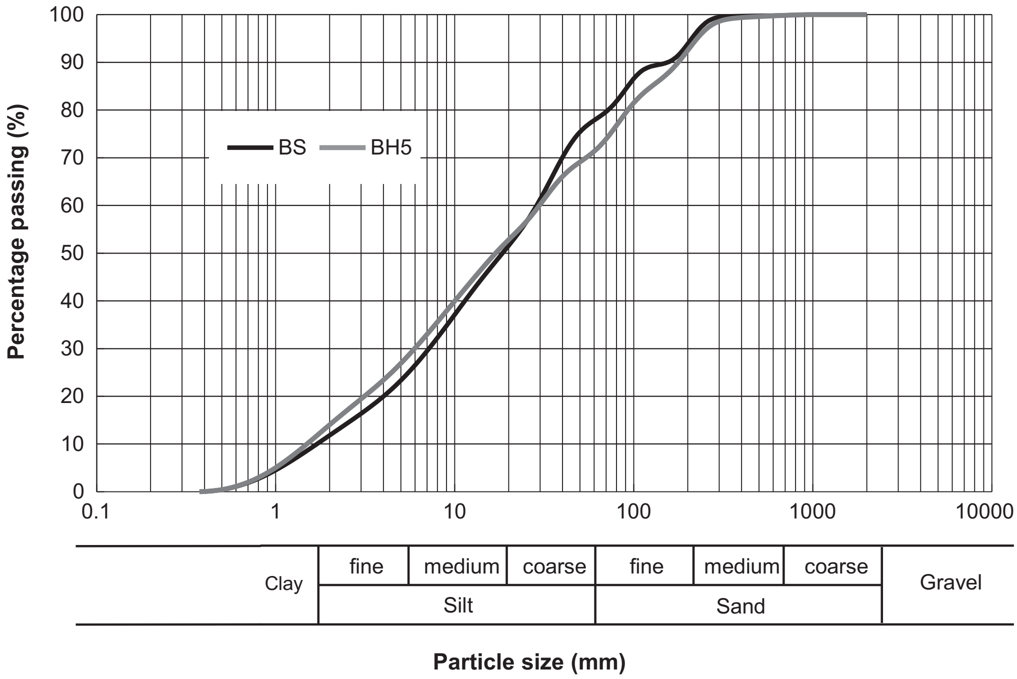

Figure 3

Figure 4

Click here to download Figure: 14_02 Carey JM_Fig_4.pdf

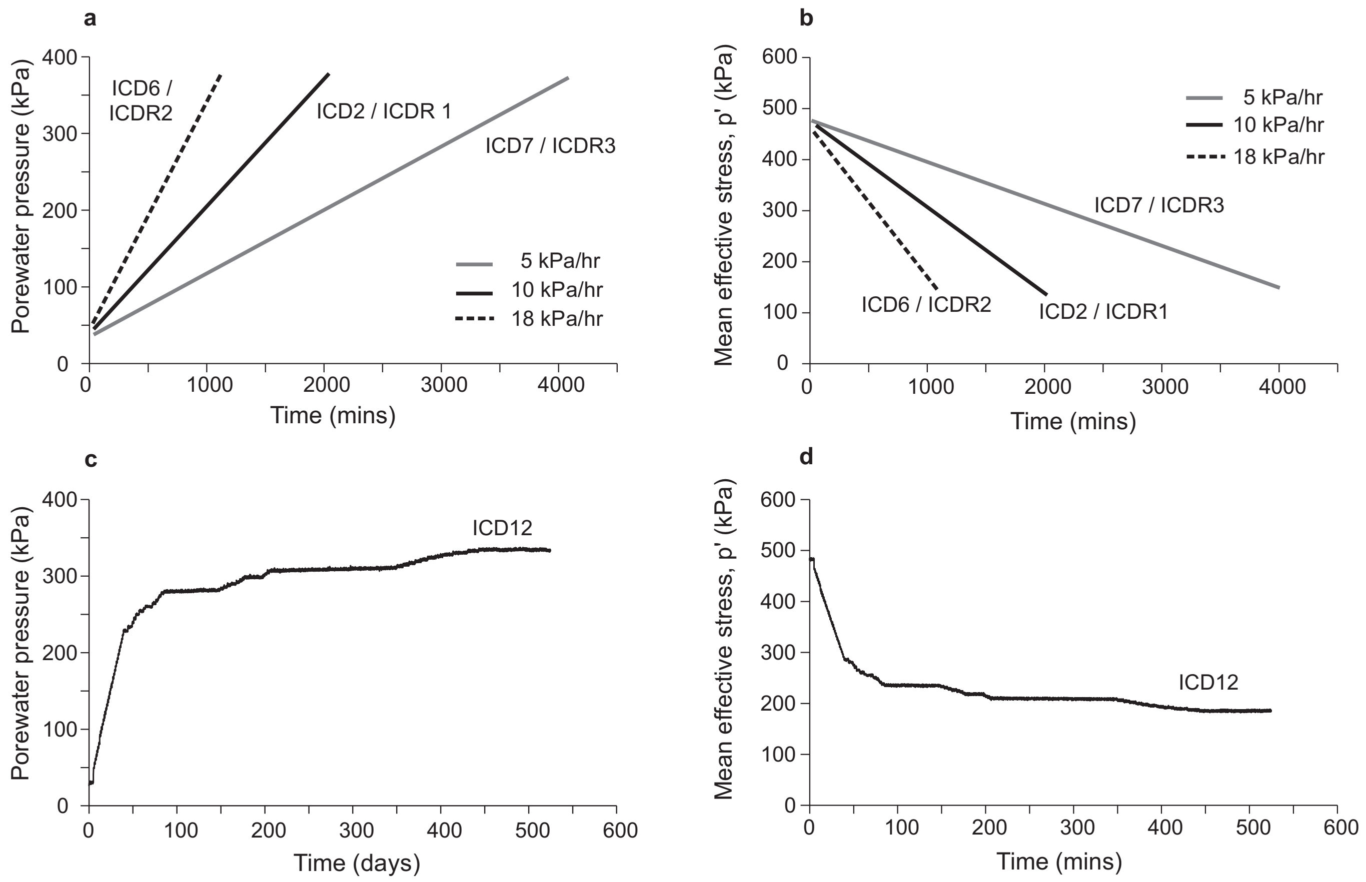

Figure 4

Figure 5

Click here to download Figure: 14_02 Carey JM_Fig_5.pdf

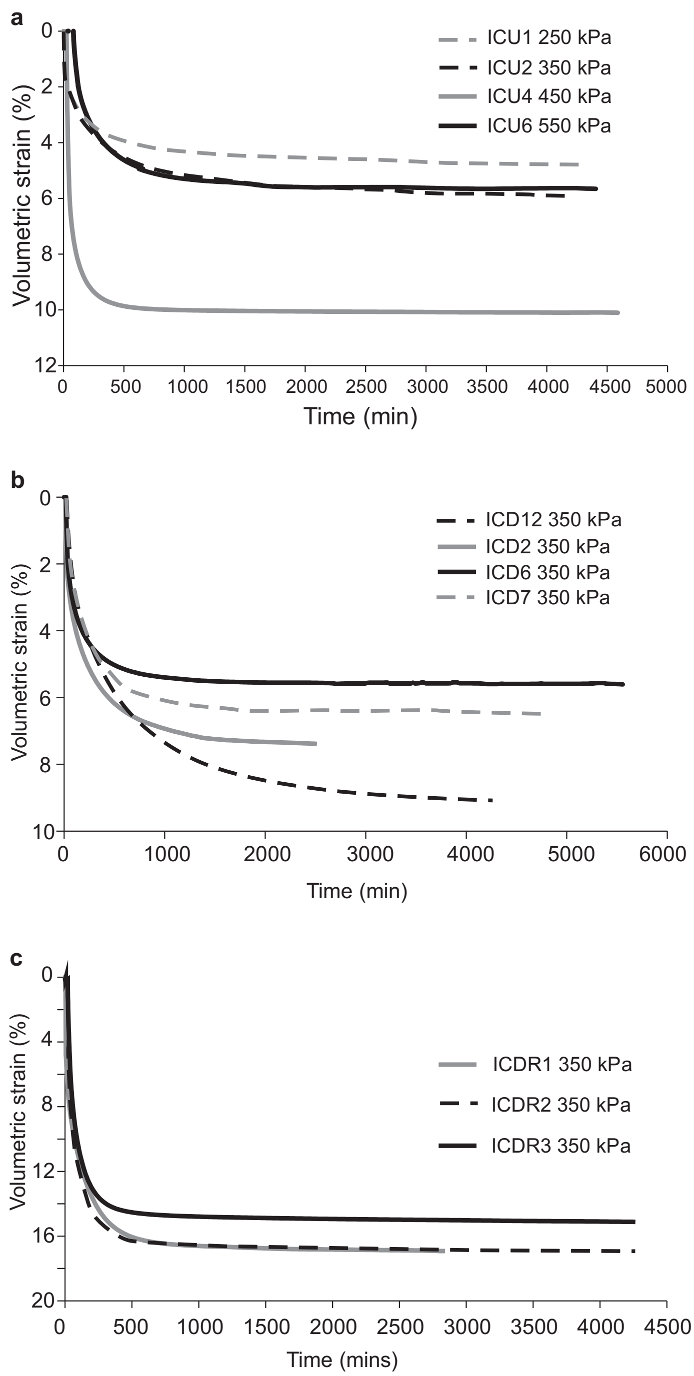

Figure 5

Figure 6

Click here to download Figure: 14_02 Carey JM_Fig_6.pdf

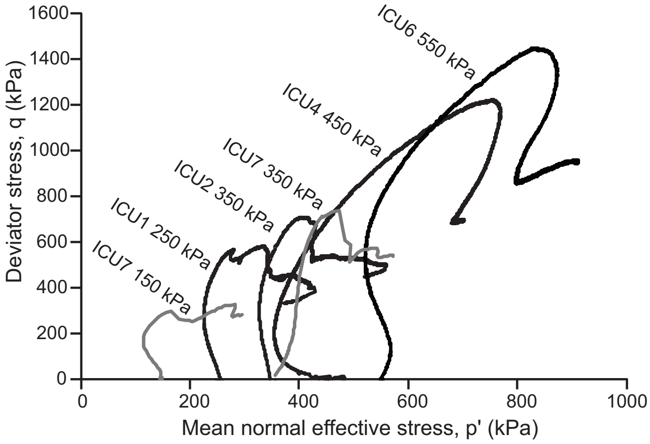

Figure 6

Figure 7

Click here to download Figure: 14_02 Carey JM_Fig_7.pdf

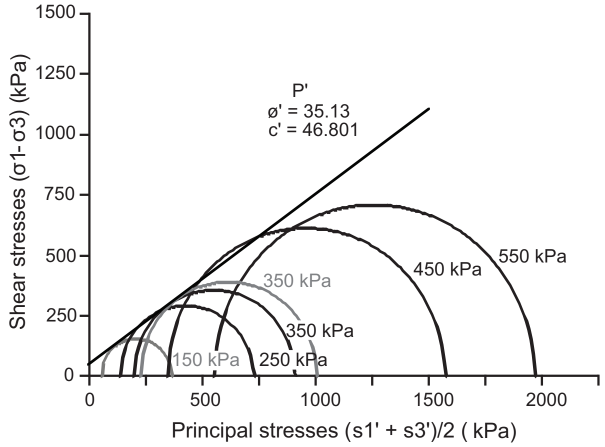

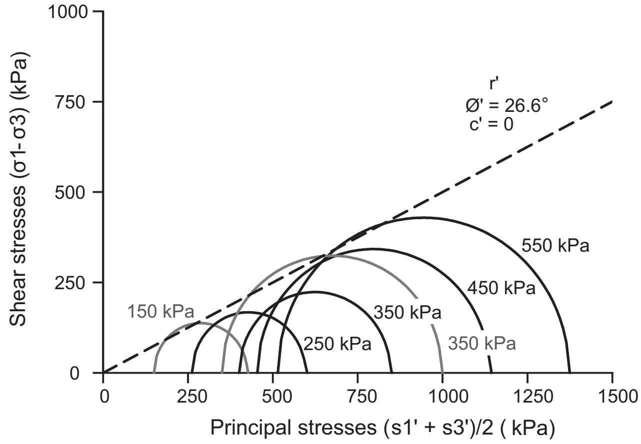

Figure 7

Figure 8

Click here to download Figure: 14_02 Carey JM_Fig_8.pdf

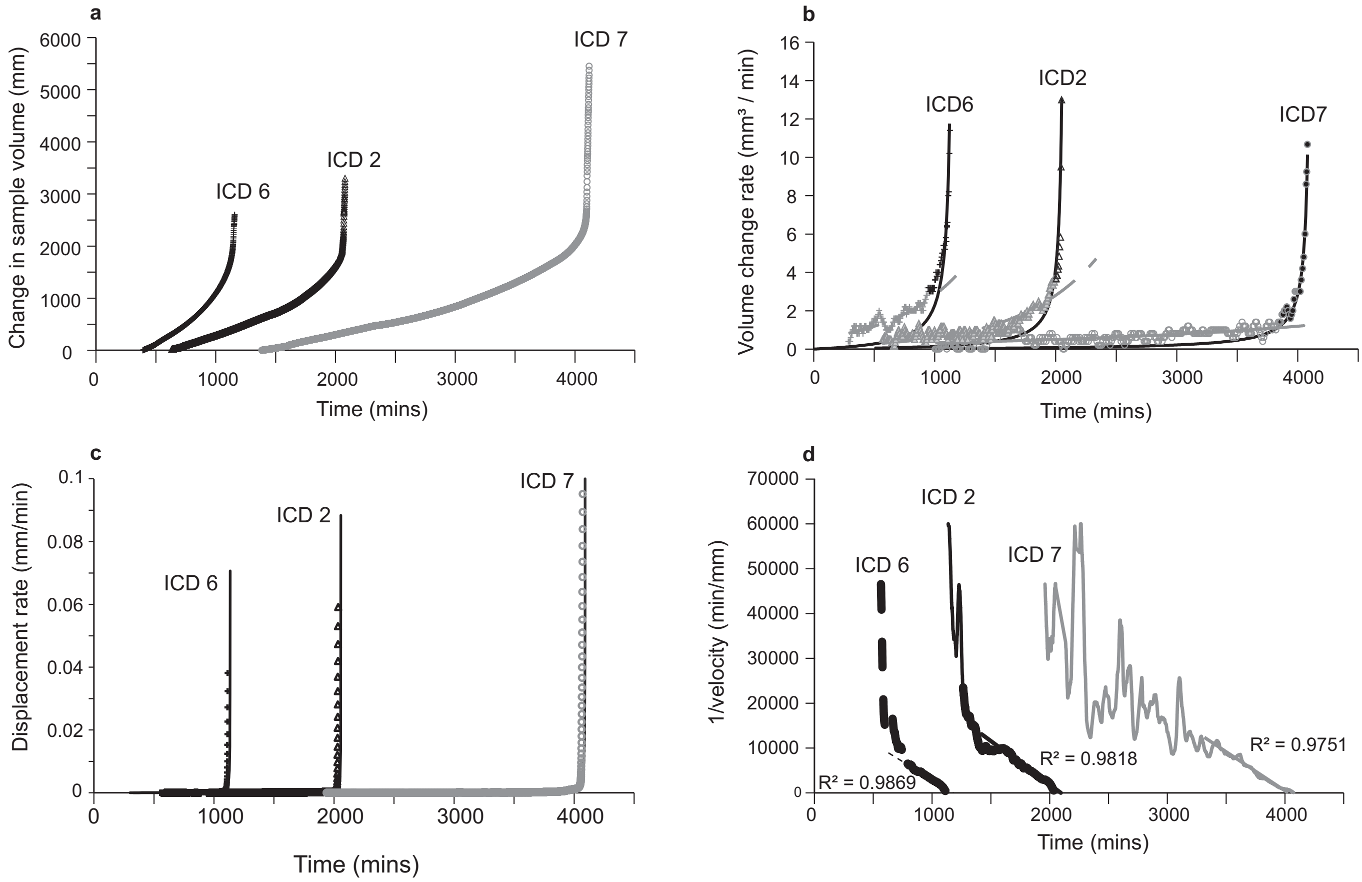

Figure 8

Figure 9

Click here to download Figure: 14_02 Carey JM_Fig_9.pdf

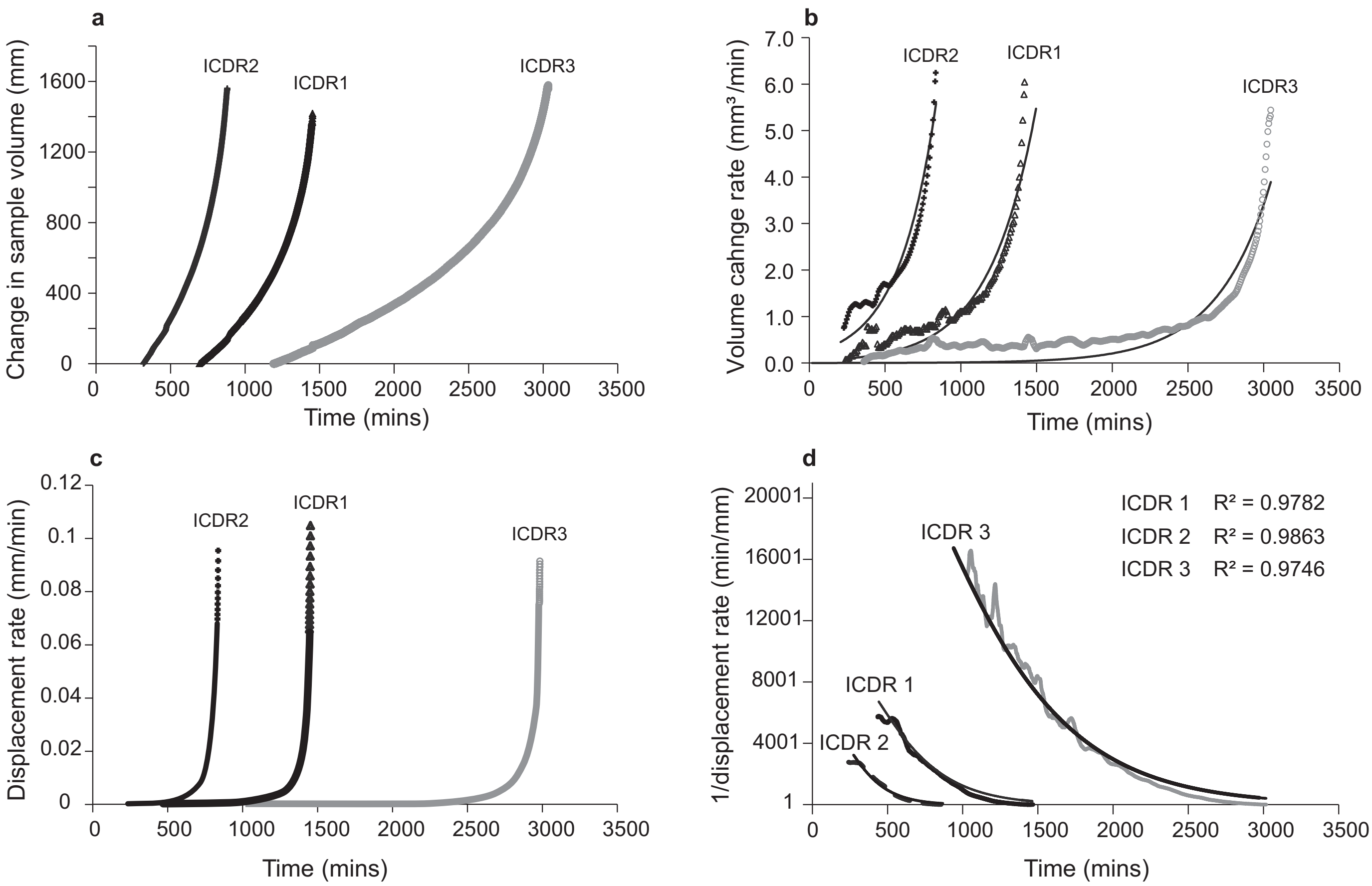

Figure 9

Figure 10

Click here to download Figure: 14_02 Carey JM_Fig_10.pdf

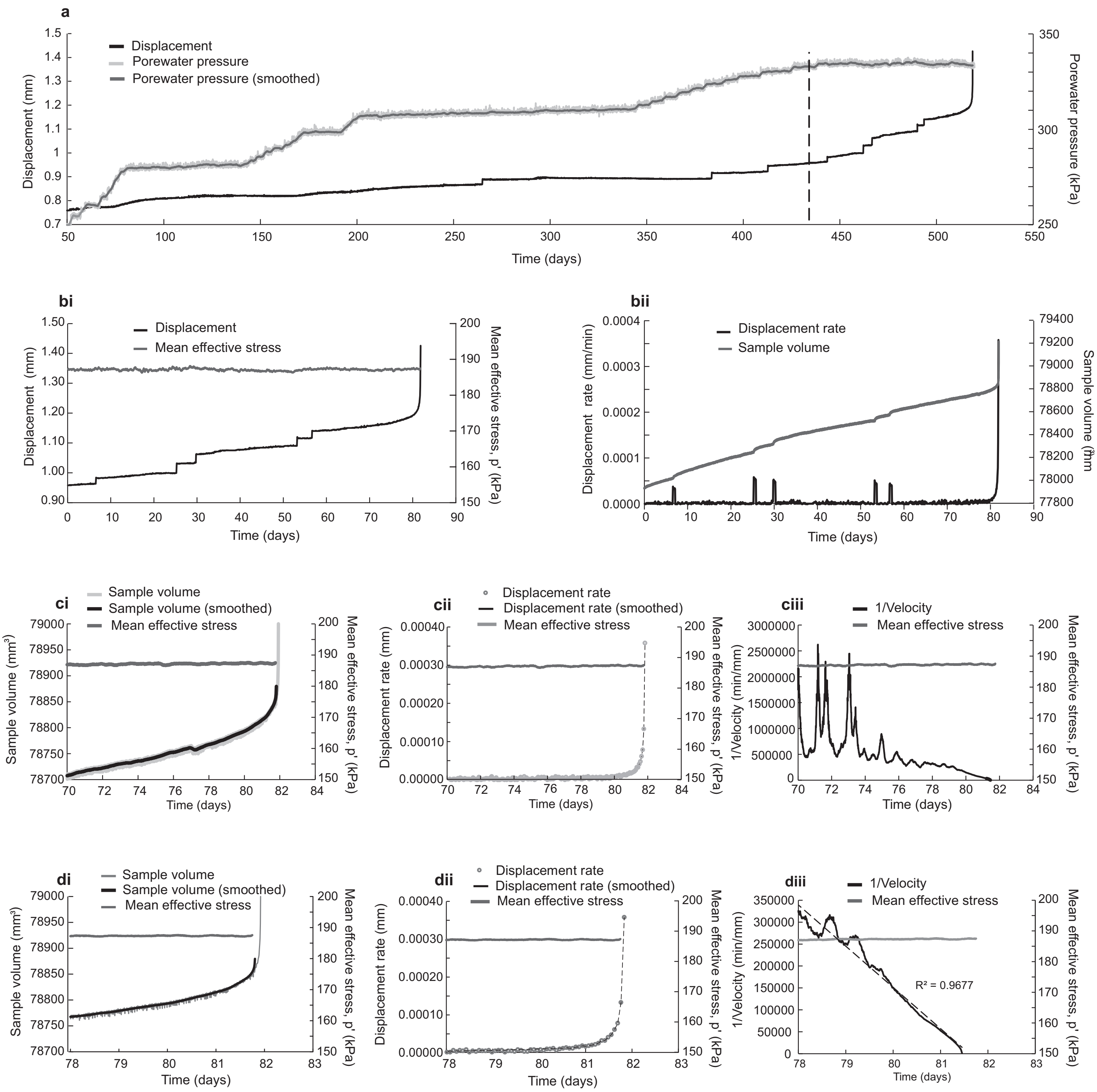

Figure 10

Figure 11
Click here to download Figure: 14_02 Carey JM_Fig_11.pdf

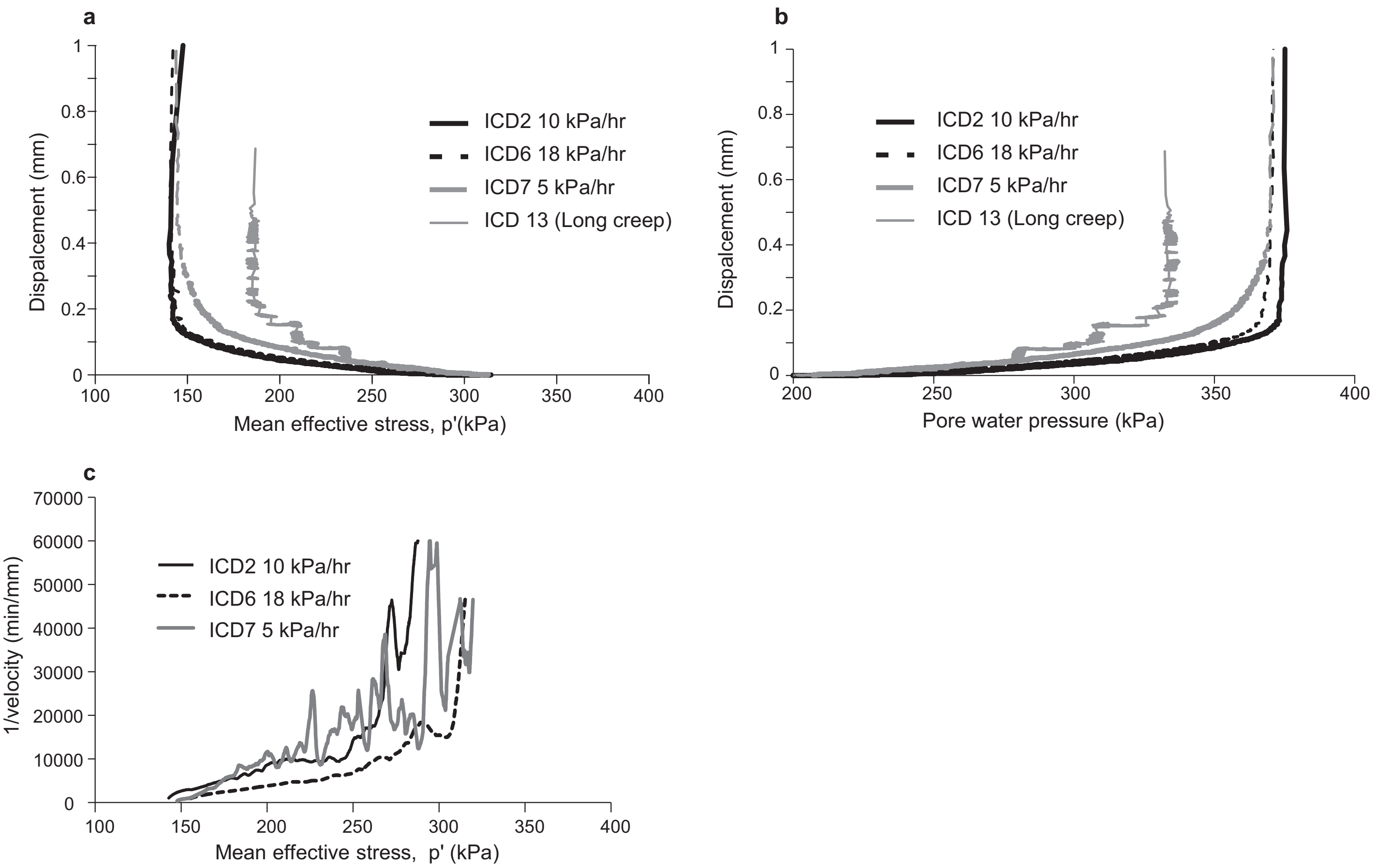

Figure 11

Figure 12
Click here to download Figure: 14_02 Carey JM_Fig_12.pdf

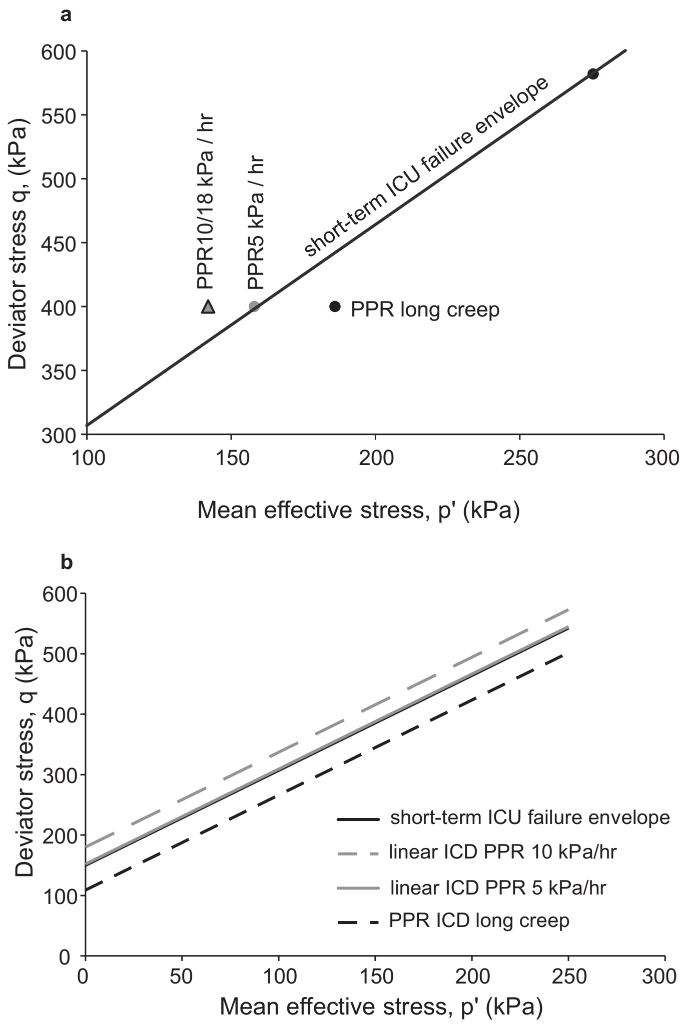

Figure 12